

## 行政院國家科學委員會專題研究計畫期中進度報告(精簡版)

計畫名稱	在四族半導體表面上的超薄離子固體自我組裝與其薄膜、介面性質 (第 2 年)		
計畫編號	NSC 5-2112-M-009-039-MY4	執行期間	2007/08/01 ~ 2008/07/31
報告類別	期中進度報告(精簡版)	計畫類別	一般型研究計畫(個別型)
計畫主持人	林登松 教授	執行單位	交通大學物理研究所
參與人員	謝明峰、馮世鑫、鐘仁陽、張展源、羅中廷		
繳交日期	2008 年 5 月 30 日		

### 目錄:

進度與結果簡要說明 .....	0
Report on “NOVEL STRUCTURE OF ULTRA THIN KCl LAYERS ON THE Si(100)-2X1 SURFACE” .....	1
I.    INTRODUCTION .....	1
II.   II. EXPERIMENTAL .....	1
III.  RESULTS .....	2
IV.  DISSCUSION .....	4
References .....	4

### 進度與結果簡要說明

今年，我們對超薄離子固體累積更多更好瞭解，我們在 NaCl 在 Ge(100)的 atomic layer epitaxy 方面獲得突破，數據已整理準備發表中。合作的理論計算 Atomic and Electronic Structures of thin NaCl films grown on the Ge(001) surface 已投稿。KCl 在 Si(100)上的成長與特性也準備發表中，第一板初稿 Novel structure of ultra thin KCl layers on the Si(100)-2x1 surface 附於後。

我們了解實驗室近期成果發表速度稍慢些，其實我們有很多很不錯的實驗結果(可在我們網頁中看到一部分尚未發表成果)，我們是希望結合理論計算結果，再完整發表好的科學論文，這種新結合(Photoemission + STM + calculation)須

要一些時間磨合，請國科會不要心急，我們設定了品質目標，也知道努力的方向。

在主計畫實驗展開與硬體設施方面，因為本計畫時期較長，國科會又加大了我們經費使用時間年度限制的彈性，而且計畫後面兩年將無新設備經費，因此我們有時間，也必須作較長遠規劃。下年度開始，我們實驗室將遷移到清華大學物理系，本計畫將隨之轉移，除了必要的一部份顯微鏡軟硬體更新與性能提升外，設備經費將保留與其他經費合併運用，這些技術上的細節我們暫且不在此報告，我們在下年度中可能會須要變更一部分設備經費運用之計畫，屆時再詳細說明我們最新的、最有效的經費運用考量。

# Novel structure of ultra thin KCl layers on the Si(100)-2×1 surface

Shiow-Fon Tsay,<sup>1</sup> J. Y. Chung,<sup>2</sup> M.-F. Hsieh,<sup>2</sup> Chun-Ting Lou,<sup>2</sup> and D.-S. Lin<sup>3,\*</sup>

<sup>1</sup>*Department of Physics, National Sun Yat Sen University,  
No. 70, Lienhai Rd., Kaohsiung 80424, Taiwan*

<sup>2</sup>*Institute of Physics, National Chiao-Tung University,  
1001 Ta-Hsueh Road, Hsinchu 30010, Taiwan and*

<sup>3</sup>*Department of Physics, National Tsing Hua University 101 Section 2 Kuang Fu Road, Hsinchu 30013, Taiwan*

(Dated: May 30, 2008)

In this paper, we investigate the growth and structure of ultra thin Potassium Chloride (KCl) films on the Si(100)-2x1 surfaces. The bonding nature between the atomic layer of ionic solid and the prototypical semiconductor surface is examined by synchrotron radiation core-level photoemission and real-time variable-temperature scanning tunneling microscopy. The Si 2p, K 3p, and Cl 2p core level spectra together indicate that interface is sharp and the ultra KCl overlayers possess similar property with the bulk KCl crystal. STM results reveal a novel c(4x4) structure at 1-ML coverage. Using DFT calculation, a model that consists of a periodical pyramidal geometry is found to accord with experimental result. In the model, the large lattice mismatch between the KCl layer and substrate causes the two dimensional ionic layer to ball up in four fold tetrahedral directions, making up the cluster array corresponding to bright protrusions in STM images.

PACS numbers: 68.35.Ct, 68.35.bj, 68.37.Ef

## I. INTRODUCTION

The nature of the solid-solid interface between very dissimilar materials has become a subject of special interest in condensed matter physics, since novel atomic and electronic structures appear at the interface. Growth of ultrathin epitaxial insulating film and the possibilities to structure these films by a self-organized process is highly important. On both semiconductors and metals, such layers are needed to separate conducting material in the ultra-small electronic devices of the future. In addition, alkali halides are often regarded as the model structure for both testing experimental methodologies and validating new theories. Thus, thin alkali halide films on semiconductors (e.g. CaF<sub>2</sub>/Si and NaCl/Ge et. al.) or on metals (e.g. NaCl/Ag, KCl/Cu, KCl/Ag, LiCl/Cu, NaCl/Cu and NaCl/Al et. al) have been regaining technological interest recently, as they are relevant for both their electronic and catalytic properties. The interesting problems include the growth mechanics, atomic and electronic structures and interface states. It also seems to affect the surface color center generation.

Thin salt films such as NaCl and KCl can grow epitaxially on Ge(001) with a high degree of quality under appropriate conditions due to the small mismatch of only 0.5% of the NaCl and Ge lattice constant. Therefore, NaCl/Ge(001) is an ideal candidate for studying the mechanisms of ionic/covalent heteroepitaxy. A wide range of experimental studies of NaCl on Ge(001) have been carried out. The remarkable and unique growth mode (carpet mode) is suggested for NaCl film of 3-8 double layers (DL) of thickness by high-resolution low-energy electron diffraction (LEED) studies. Experimental results also suggest that the subsequent growth of NaCl on the modified surface occurs through the formation of islands with the thickness of a triple-layer, which fills in un-

til the triple-layer is complete. A well-resolved square lattice with a lattice constant of 4.0 Å STM image is observed, and Glockler et al. suggested that only one type of ions (Na<sup>+</sup> or Cl<sup>-</sup>) of the NaCl(001) plane is imaged as white protrusions. On the other hand, the NaCl/Ge interface should play an important role for the growth mode, but only a few experiments have studied the properties of buried interfaces. This is due to the instability of alkali halides surface during electron irradiation. Lucas et al. found that the c(4x2) surface reconstruction, a characteristic of clean Ge(001) at low temperatures, is suppressed immediately upon deposition of NaCl, (not clear, do you mean: (2x1) symmetric surface structure, another kind of reconstruction of clean Ge(100) was observed after growth of NaCl film up to 6 ML.) instead of preserving the (2x1) symmetry surface structure, even after 6 monolayers (ML) of NaCl film has been grown. Zielasek et al. found the electronic states located at the interface in electron energy loss scattering (EELS) measurement, and suggested that the dimerization of the Ge(001) surface not be removed at the NaCl/interface even if the thickness of NaCl is up to 20 ML.

Several problems about the structural and electronic properties of this system such as atomic adsorption sites, charge transfer of interfaces, and the nature of the interface, are under debate. Until now, the theoretical models are lacking for completely describing the epitaxial growth mechanism.

## II. EXPERIMENTAL

The Si(100) samples were sliced from Antimony doped with the resistance of 0.01 Ω-cm. After thorough outgassing at ~900 K, the dimerized clean Si(100) surface was obtained by feedback-controlled heating to ~1450 K

for a few seconds. After direct heating, KCl of 99.99% purity was evaporated from an alumina crucible by a feedback controlled electron bombardment beam. The deposition rate was measured by an integral flux monitor calibrated by a quartz-crystal thickness monitor. The substrate temperature during growth was about 330 K.

The photoemission spectra were observed at the Taiwan Light Source laboratory in Hsinchu, Taiwan. Synchrotron radiation from a 1.5-GeV storage ring was dispersed by a wide-range spherical grating monochromator (SGM). The photocurrent from a gold mesh positioned in the synchrotron beam path was monitored to measure the relative incident photon beam flux. Photoelectrons were collected  $15^\circ$  from  $60^\circ$  off normal emission and analyzed by a 125-mm hemispherical analyzer in a  $\mu$ -metal shielded UHV system. The overall energy resolution was less than 120 meV. The STM measurement was performed in a separated UHV chamber.

### III. RESULTS

#### A. Photoemission results

High-resolution core level photoemission spectroscopy can be used to distinguish atoms at nonequivalent sites and in different chemical bonding configurations, according to shifts in their binding energy.<sup>17</sup> In the following analysis of the Si and Cl 2p core level spectra, we use Voigt line shapes that consist of component of spin-orbit split doublets is assumed to have the same Figures 1(a) and 1(b) show the respective surface-sensitive Si 2p and Cl 2p core-level spectra (circles) for Chlorine terminated Si(100)-2 $\times$ 1 surface and clean Si(100) covered with various amount of KCl. The coverage was expressed in terms of Si(100) monolayers (ML), and 1 ML =  $6.78 \times 10^{14}$  atoms/cm<sup>2</sup>. The bottom Cl 2p spectrum in Fig. 1(b) spectra in Fig. 1(b) can be analyzed with only one component that consists of a pair of split doublets separated by 1.60 eV. The bottom spectrum in Fig. 1(a) displays the Si 2p core level spectra for the Cl-Si(100)-2 $\times$ 1 surface. This Si 2p spectrum consists of two components, B and Si<sup>+</sup>, separated by about 0.90 eV. The B component was responsible for emission from the bulk and the Si<sup>+</sup> component from the surface Si-Cl species.<sup>19</sup> All fitting was least-squares fitting.<sup>18</sup> The results of the fits are indicated by the solid curves overlapping the data points.

The results in Figs. 1(a) and 1(b) show that the integrated intensities of Cl 2p spectra increase at the expense of Si 2p, indicating that KCl films grow epitaxially. The second lowest Si 2p spectrum obtained from a clean Si(100) surface exhibits a prominent peak S at the low binding energy side. This component has been attributed to emission from up atoms of asymmetric dimers. At sub-monolayer coverage of KCl, the intensity of the S component in spectra decreases progressively, indicating that the up atoms in the dimerized layer lose their negatively charged characteristics upon adsorption of KCl. The tail

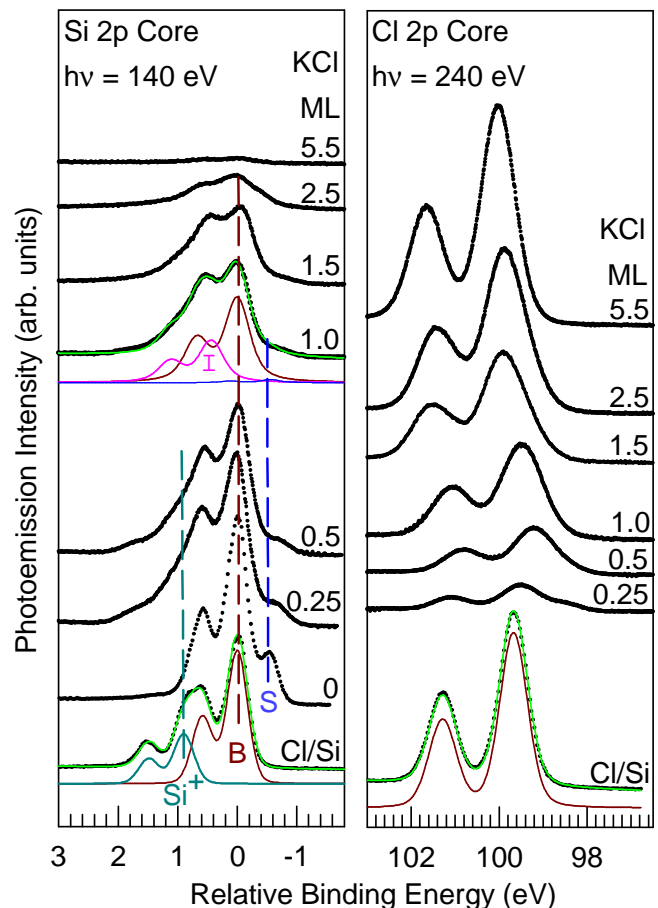


FIG. 1: The (a) Si 2p and (b) Cl 2p core level photoemission spectra (circles) for the Cl-Si(100)-2 $\times$ 1 surface and the Si(100) surface with various amounts of KCl deposition as labeled. The solid curves are fits to the spectra. The curves labeled B, S, I and Si<sup>+</sup> are the results of decomposition of the Si 2p spectra into contributions from the bulk, clean surface, interface layer, and Si-Cl species, respectively. The energy zero in (a) refers to the  $2p_{3/2}$  bulk position. To eliminate the band bending effect, the relative binding energy for the Cl 2p refers to the corresponding Si  $2p_{3/2}$  line of the B component in (a). Dash lines are shown through the B, S, and Si<sup>+</sup> components as a guide to the eye.

on the higher binding energy side for Si 2p with 0.25 and 0.5 ML KCl coverage locate near the position of the Si<sup>+</sup> component, indicating that a portion of adsorbed KCl molecules decomposes and Si-Cl bonds are presented on the surface. The

Figure 2 plots the integrated intensities of the Cl 2p spectra ( $I_{Cl}$ ), which is proportional to the surface Cl coverage. The integrated intensity of the bottom spectrum is normalized to be 1.0 because the chlorine coverage is nominally 1 ML for the Cl-saturated Si(100) surface before H-atom bombardment.  $I_{Cl}$  decreases linearly with the dosage of H-atoms at the early stage, indicating that Cl atoms were removed by impinging H atoms. This result is consistent with a previous study.<sup>11</sup>

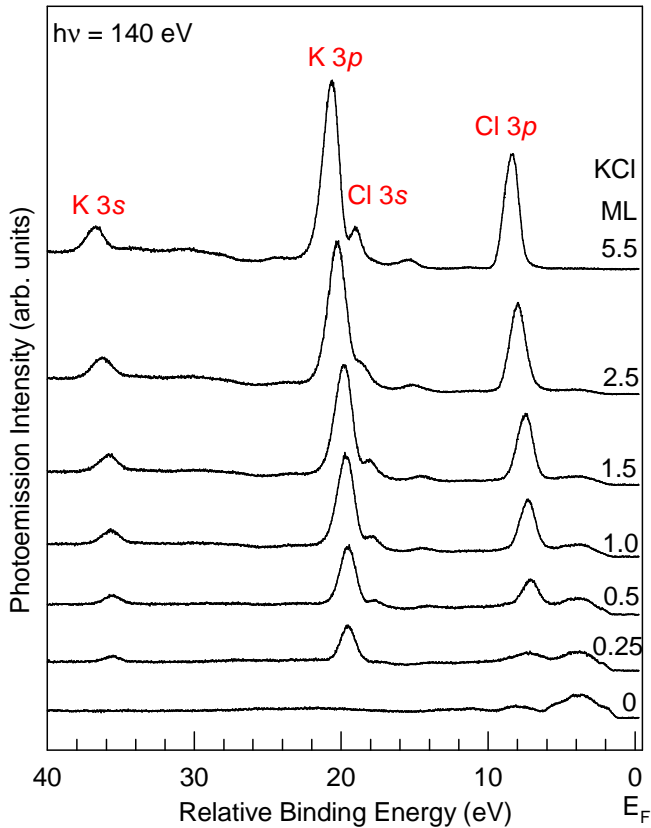


FIG. 2: The valence band region of the Si(100) surface with various KCl coverage as indicated. Similar to Fig. 1(b), the relative binding energy refers to the corresponding Si  $2p_{3/2}$  line of the B component in Fig. 1(a). The vertical dash lines are guide to the eye to show the general trend in the binding energy shifts of K  $2p$  and Cl  $3p$ .

As the exposure of atomic hydrogen increases, both the intensities of the Si<sup>+</sup> component and the Cl  $2p$  spectra drop off. This occurrence suggests that H atoms reduce the surface Cl coverage, as a previous report has found.<sup>11</sup> After >1000 L of apparent exposure, the line shape of Si  $2p$  is similar to that (top spectrum in Fig. 1(b)) obtained by direct, high-dosage hydrogen exposure on the clean Si(100)- $2\times 1$  surface at room temperature.<sup>20</sup> This observation indicates that hydrogen atoms terminate nearly all surface dangling bonds and form a mixture of dihydride and monohydride surface when most Cl atoms are extracted. Note that a small component labeled Si<sup>2+</sup> emerges in Fig. 1(b) after H impingement. The chemical shift of Si<sup>2+</sup>, around 1.78 eV on the higher bonding energy side of B, is consistent with a charged state of +2 for Si atoms and responsible for SiCl<sub>2</sub> species.<sup>14</sup> Presumably, the SiCl<sub>2</sub> species were formed as a consequence of the highly exothermic uptake of halogens during the extraction. Although more study is needed, the emergence of the dichloride species implies that impinging H atoms induce other surface reactions besides extracting upon collision with a surface adatom.

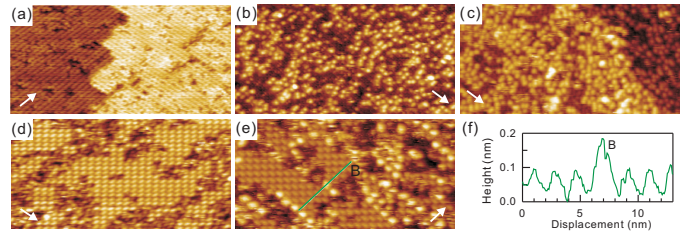


FIG. 3: STM images showing the coverage evolution with (a) 0.1-, (b) 0.3-, (c) 0.5-, (d) 0.8-, and (e) 1.2-ML KCl deposition on the Si(100)- $2\times 1$  surface. The sample bias used was  $-2.3$  —  $-2.5$  V. The images cover an area of about  $40\times 20$  nm<sup>2</sup>. The white arrows indicate the dimer-row direction in the top silicon layer. (f) The apparent topographic height profile taken along the green line marked in (e).

## B. STM results

The clean double-domain Si(100) surface consists of rows of dimers; the two dangling bonds from the two atoms in a dimer form a weak pi-bond.<sup>21</sup> Figures 3 and 4 show the evolution of the Si(100) surface after KCl deposition at about 330 K. In Fig. 3 the dimer-row directions in the top Si layer before deposition are indicated by white arrows. Upon small amount of KCl adsorption, noisy images resulting from the often unstable feedback loop were observed. Besides a handful of dark sites on the dimerized surface as shown in better images such as Fig. 3a, no apparent KCl adsorption species are discerned at coverage below 0.2 ML. The unstable scans and fewer-than-expected apparent adsorption species together indicate that the deposited KCl molecules at low coverage are not strongly chemisorbed and likely quite mobile on the clean Si surface. As KCl adsorption accumulates to near 0.3 ML, random bright protrusions develop and grow in numbers as Fig. 3(b) and 3(c) show. Larger than atomic sizes and not observed at  $\leq 0.2$  ML, these protrusions are likely nucleated clusters of KCl formed after critical supersaturation.<sup>1</sup>

At above 0.6 ML, well-ordered  $c(4\times 4)$  arrays of protrusions appear and grow in size amid the disordered clusters as Fig. 4(a) and Fig. 3(d) display. Each of the  $c(4\times 4)$  cells consists only one elongated elliptical protrusion as which semimajor axis is perpendicular to the substrate dimer-row direction. While the atomic features are not resolved, the size of these protrusions suggests that each protrusion is the collective feature of a KCl-substrate cluster, denoted as Cluster A. At around 1.0 ML the  $c(4\times 4)$  domains expand to fill the terraces as Fig. 4(b) shows. As Figs. 3(d) and 3(e) depict, the fragmented  $c(4\times 4)$  areas are separated by domain boundaries that possess of no apparent atomic ordering. Above 1 ML coverage, clusters of a new kind (denoted as Cluster B) appearing as bright protrusions in Fig. 3(e) and 4(b). Cluster B randomly disperse in the area of domain boundaries and often form linear chains on top of  $c(4\times 4)$  regions. As KCl deposition continues, STM images such

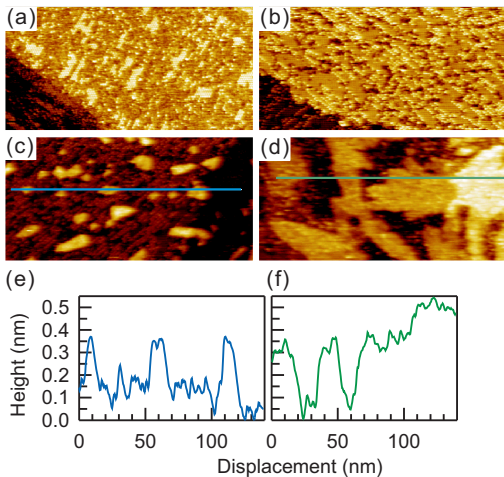


FIG. 4: Large area STM images ( $200 \times 100 \text{ nm}^2$ ) showing the coverage evolution with (a) 0.6-, (b) 1.2-, (c) 2.4-, and (d) 3.6-ML KCl deposition on the Si(100)- $2 \times 1$  surface. The sample bias used was  $-2.3 \text{ V}$ . The islands in (c) have an apparent height of about  $1.7 \text{ \AA}$ . (e) and (f) are apparent topographic height profiles taken along horizontal lines marked in (c) and (d), respectively.

as Figs. 4(c) and 4(d) show that the two dimensional island growth multilayer growth is followed and above 2 ML, images up to 2 ML coverage

#### IV. DISCUSSION

The calculations of total energy were performed using VASP code<sup>20-22</sup> within LDA of DFT. The Ceperley-Alder<sup>23</sup> exchange-correlation function, as parameterized by Perdew and Zunger, was adopted. A repeated-slab supercell model was employed. Each slab includes ten atomic layers of Ge and the adlayers of Na and Cl; H atoms are attached to the bottom-layer Ge atoms to saturate their dangling bonds. The heights of the supercell in the  $[001]$  direction were fixed to  $6 \text{ nm}$ , which was sufficiently large to prevent coupling between the slabs even for the Na, Cl and H adsorbed on both Ge surfaces. The wave functions were expanded using a plane-wave basis with an energy cutoff of  $25.72 \text{ Ry}$  ( $350 \text{ eV}$ ). The electron-ion interaction pseudopotentials supported by VASP were specified using the projector-augmented wave (PAW) method,<sup>25</sup> in which the  $2p$  and  $3s$  electrons of the Na atom, the  $3s$  and  $3p$  electrons of the Cl atom,

and  $3d$ ,  $4s$  and  $4p$  electrons of the Ge atom are considered the valence electrons. The calculated lattice parameter of bulk Ge was  $5.621 \text{ \AA}$  which included a  $0.6 \%$  error from the experimentally determined value. An  $88 \text{ k}$  ( $4 \times 4$ ) Monkhorst and Pack mesh, equivalent to  $32$  ( $8$ )

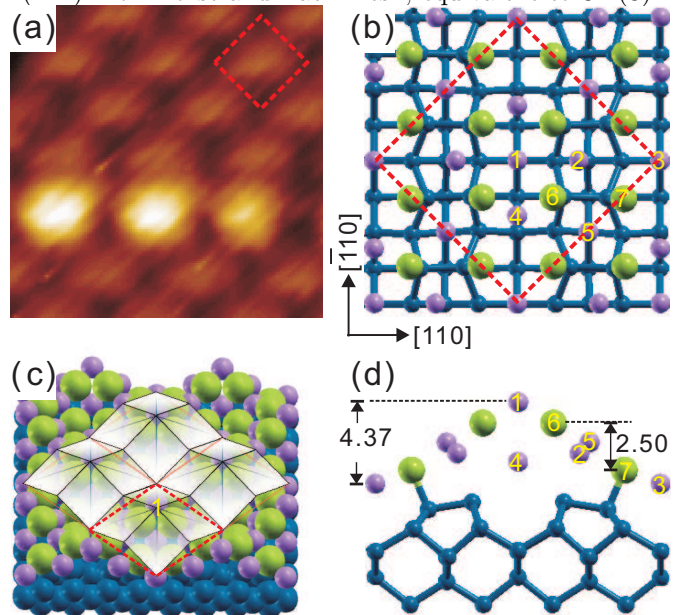


FIG. 5: (a) Close-up image of the  $c(4 \times 4)$  structure shown in Fig. 4(b). The red rectangle denotes the unit cell of the ordered clusters. The bright protrusions on the lower area are Cluster B. (b) Top, (c) perspective, and (d) side view through atoms 1 and 2 in (b) of the atomic model of the  $c(4 \times 4)$  structures. Blue, green, and purple circles indicate Si, Cl, and Na atoms, respectively.

irreducible  $k$  points, was used to sample the surface Brillouin zone of a  $(4 \times 4)$  unit cell. By fixing the bottom double Ge and H layers, the structure was optimized until the residual force acting on each atom was less than  $0.01 \text{ eV/\AA}$ .

#### Acknowledgments

This work is supported by the National Science Council of Taiwan under Contract No. NSC 95-2112-M009-0039-MY4 (DSL) and NSC 95-2112-M-110 -016 -MY3 (SFT) and by the National Synchrotron Radiation Research Center and National Center for High-Performance Computing.

\* Electronic address: ds1in@phys.nthu.edu.tw

<sup>1</sup> Surface Science: an introduction, J. B. Hudson

(Butterworth-Heinemann, Boston, 1991), PP. 289.

<sup>2</sup> J. G. Quattrucci and B. Jackson, J. Chem. Phys. **122**,

- 074705 (2005).
- <sup>3</sup> C. T. Rettner and D. J. Auerbach, *Phys. Rev. Lett.* **74**, 4551(1995).
  - <sup>4</sup> S. A. Buntin, *J. Chem. Phys.* **108**, 1601 (1998).
  - <sup>5</sup> C. T. Rettner, *J. Chem. Phys.* **101**, 1529 (1994).
  - <sup>6</sup> D. D. Koleske and S. M. Gates, *J. Chem. Phys.* **99**, 8218 (1993).
  - <sup>7</sup> S. M. Gates, *J. Phys. Chem.* **96**,10439 (1992).
  - <sup>8</sup> K. R. Lykke and B. D. Kay, in *Laser Photoionization and Desorption Surface Analysis Techniques*, Edited by N. S. Nogar (SPIE, Bellingham, WA, 1990), Vol. **1208**, p. 18.
  - <sup>9</sup> B. Jackson, X. Sha, and Z. B. Guvenc, *J. Chem. Phys.* **116**, 2599 (2002).
  - <sup>10</sup> C. M. Aldao and J.H. Weaver, *Prog. in Surf. Sci.* **68**, 189 (2001), and reference therein.
  - <sup>11</sup> C. C. Cheng, S. R. Lucas, H. Gutleben, W. J. Choyke, and J. T. Yates, Jr., *J. Am. Chem. Soc.* **114**, 1249 (1992); *ibid* *Surf. Sci.* **273**, L441 (1992).
  - <sup>12</sup> Y. H. Kim, J. Ree, and H. K. Shin, *J. Chem. Phys.* **108**, 9821 (1998).
  - <sup>13</sup> K. Hattori, K. Shudo, M. Ueta, T. Iimori, F. Komori, *Surf. Sci.* **402-404**, 170 (1998).
  - <sup>14</sup> M.-W. Wu, S.-Y. Pan, W.-H. Hung, and D.-S. Lin, *Surf. Sci.* **507**, 295 (2002).
  - <sup>15</sup> H. N. Waltenburg and J. T. Yates, Jr., *Chem. Rev.*, **95**, 1589 (1995).
  - <sup>16</sup> Q. Gao, C. C. Cheng, P. J. Chen, W. J. Choyke, and J. T. Yates Jr., *Thin Solid Film* **225**, 140 (1993).
  - <sup>17</sup> F. J. Himpsel, F. R. McFeely, J. F. Morar, A. Taleb-Ibrahimi, and J. A. Yarmoff, in *Photoemission and Adsorption Spectroscopy of Solids and Interfaces with Synchrotron Radiation*, Proceedings of the International School of Physics "Enrico Fermi", Course CVIII, edited by G. Scoles (North-Holland, New York, 1991).
  - <sup>18</sup> T.-C. Chiang, *CRC Crit. Rev. Solid State Mater. Sci.* **14**, 269 (1988).
  - <sup>19</sup> D.-S. Lin, J. L. Wu, S.-Y. Pan, and T.-C. Chiang, *Phys. Rev. Lett.* **90**, 046102 (2003).
  - <sup>20</sup> K. Yamamoto and M. Hasegawa, *J. Vacuum Sci. Technol. B* **12**, 2493 (1994).
  - <sup>21</sup> J. J. Boland, *Adv. Phys.* **42**, 129 (1993) and references therein.
  - <sup>22</sup> I. Lyubinetsky, Z. Dohnalek, W. J. Choyke, and J. T. Yates, *Phys. Rev. B* **58**, 7950 (1998).
  - <sup>23</sup> G. J. Xu, K.S. Nakayama, B. R. Trenhaile, C. M. Aldao, and J. H. Weaver, *Phys. Rev. B* **67** 125321 (2003).
  - <sup>24</sup> B. R. Trenhaile, V. N. Antonov, G. J. Xu, A. Agrawal, A.W. Signor, R. Butera, K. S. Nakayama, and J. H. Weaver, *Phys. Rev. B* **73**, 125318 (2006).
  - <sup>25</sup> J. H. G. Owen, D. R. Bowler, C. M. Goringe, K. Miki, and G. A. D. Briggs, *Phys. Rev. B* **54**, 14153 (1996).
  - <sup>26</sup> J. Trost, T. Zambelli, J. Wintterlin, and G. Ertl, *Phys. Rev. B* **54**, 17850 (1996).
  - <sup>27</sup> There exists a possibility that the trajectory of an incoming H atom is slightly redirected by the Cl-extracted site to its close vicinity. However, our calculation based on the classical electrostatic force from surface dipoles suggests that the deflection is too small.